



## EXPERIMENTAL INVESTIGATION OF FABRIC REINFORCED CEMENTITIOUS MATRIX FOR STRENGTHENING OF INFILL WALLS

S Lalit Sagar<sup>(1)</sup>, V. Singhal<sup>(2)</sup>, D. C. Rai<sup>(3)</sup>

<sup>(1)</sup> Former Graduate Student, Department of Civil Engineering, Indian Institute of Technology Kanpur, Kanpur, UP, 208016, India

<sup>(2)</sup> Assistant Professor, Department of Civil and Environmental Engineering, Indian Institute of Technology Patna, Bihta, Bihar, 801103, India, singhal@iitp.ac.in

<sup>(3)</sup> Professor, Department of Civil Engineering, Indian Institute of Technology Kanpur, Kanpur, UP, 208016, India, dcrai@iitk.ac.in

### **Abstract**

Strengthening of masonry infills is essential to mitigate their brittle failure especially in the out-of-plane direction during earthquakes. Light weight composite materials such as fiber reinforced polymer (FRP) have been popularly used in different forms for seismic upgradation of masonry infilled reinforced concrete (RC) frames. However, owing to the disadvantages posed by the use of the organic binders in these composite systems, the feasibility of replacing them with inorganic matrices to enhance their overall efficiency has been evaluated in this study.

An experimental program has been conducted to evaluate the bidirectional behavior of masonry infilled RC frames strengthened using glass Fabric Reinforced Cementitious Matrix (FRCM). Six half-scale masonry infilled RC frames with different FRCM configurations were tested to study the effect of method of the fabric application, provision of mechanical anchors and the orientation of fiber strands on the performance of the strengthened infill walls. Two modes of wet lay-up application which differ in the sequence of placing the fabric have been studied. A unique loading protocol was used for bidirectional loading of the specimen, consisting of successive application of slow cyclic drifts for in-plane loading and shake-table generated ground motion for out-of-plane loading.

FRCM strengthening improved the strength and ductility of the masonry infills. The strengthened infill walls could safely withstand a drift in excess of 2.20%, preserving the structural integrity without jeopardizing its out-of-plane capacity. The direct mode of application of the fabric, where the fabric was applied directly on the infill wall exhibited a superior performance compared to sandwich application, where the fabric was embedded between two layers of mortar. The direct mode of application helped delay the onset of cracking in the infill walls, and showed better deformability with about 30% higher yield displacement compared to the sandwich mode. The mechanical anchors were effective in limiting the separation of the infill panel from the frame, resulting in a better bidirectional response of the infill wall. The anchored specimens showed superior post-peak behavior, due to the improved load sharing between the infill and the boundary frame which prevented the abrupt drop in the in-plane loads with the development of shear cracks at the column ends.

*Keywords: Masonry infill; Fabric Reinforced Cementitious Matrix; Shake table test; Seismic strengthening*



## 1. Introduction

Reinforced concrete (RC) construction with masonry infill walls is one of the most widely practiced construction typologies across the world. Though the infills are helpful in increasing the lateral stiffness of the structure and attaining higher energy dissipation, its brittle nature and poor bond with the surrounding frame, makes it vulnerable to collapse during a seismic event. In the earlier studies, masonry structures strengthened with fiber reinforced polymer (FRP) sheets and rods have shown considerable improvements in strength and ductility over the unstrengthened specimens [1, 2]. Despite its ability in enhancing the performance of masonry wallets, it suffers from drawbacks such as poor durability, inability to apply on wet surfaces, and other problems associated with the use of organic binders [3-6]. In order to increase the scope of utility of FRP sheets in practical applications, the organic binder has been replaced with cementitious matrix to improve the bond, durability and fire resistance of the strengthening system. The resulting composite material is known as fabric reinforced cementitious matrix (FRCM).

Past experimental studies suggests that the FRCM strengthened masonry wallets tested under in-plane shear and out-of-plane flexural loads have shown considerably good performance [6-9] and have been able to match their FRP strengthened counterparts in terms of ultimate strength, ductility, post-peak behavior, etc [4, 5]. Though FRCM has been proven to be effective in strengthening of masonry wallets, there have been very few attempts to study the behavior of FRCM strengthened infilled RC frames, especially under dynamic loads [10]. In this study, the bidirectional behavior of the infill wall has been studied under a unique loading protocol developed by Komaraneni et al. [11].

In the earlier experimental investigations, FRCM strengthening of masonry surfaces was performed by embedding the FRP sheets between two layers of cement mortar, which is analogous to the epoxy based strengthening. However, in the present study the efficacy of a novel strengthening technique where the FRP sheet is placed directly on the surface of masonry, referred to as the direct application has been evaluated in comparison to the conventional method, referred to as the sandwich application. Also, the contribution of mechanical anchors in improving its interaction between the RC frame and masonry has been investigated. Further, the separation of infill wall is followed by the formation of the diagonal strut mechanism where the load is transferred along the diagonals. So, the effect on the performance of FRCM strengthening system with the change in the orientation of the fiber strands has also been evaluated.

Therefore, the key objectives of the present experimental study were to evaluate the efficacy of two FRCM strengthening techniques which differ in the sequence of placing the fabric, to study the contribution of mechanical anchors in enhancing the efficiency of the strengthening system, and the effect of orientation of the fiber strands on the performance of the infilled RC frames under bidirectional loading.

## 2. Experimental Program

### 2.1 Test Specimens

The experimental program consisted of six half-scale clay brick masonry infill walls. The geometric and reinforcement details for the typical RC frame with infill are given in Fig. 1. Plaster of thickness 6 mm was applied on either face of the wall, and the overall thickness of the wall was 76 mm. The reinforced concrete (RC) frame was designed as an ordinary moment resisting frame (OMRF) with no special confining reinforcement.

In the test matrix, first specimen was the unstrengthened or control specimen and the remaining specimens were strengthened with different FRCM configurations. The specimen is denoted using alphanumeric symbol as  $XY_N$  where X denotes the mode of fabric application (D for direct application and S for sandwich application), Y denotes the use of anchors (A for anchored and U for unanchored) and subscript N denotes the angle of orientation of fiber strands with respect to the bed-joint ( $0-90^\circ$  or  $\pm 45^\circ$ ). The details of the strengthening configuration along with the symbols used are presented in Table 1. In the direct mode of application, the fabric was placed on the surface of masonry directly, and then coated with a single mortar layer of 6 mm thickness. Whereas in sandwich mode of application, the fabric was placed between two mortar layers of 2 mm and 4 mm

thicknesses. The configuration for the last specimen DA<sub>45</sub> was selected based on the test results of the four strengthened specimens, and subsequently direct mode of application with anchors was selected, with fiber orientation of  $\pm 45^\circ$  with respect to the bed-joint.

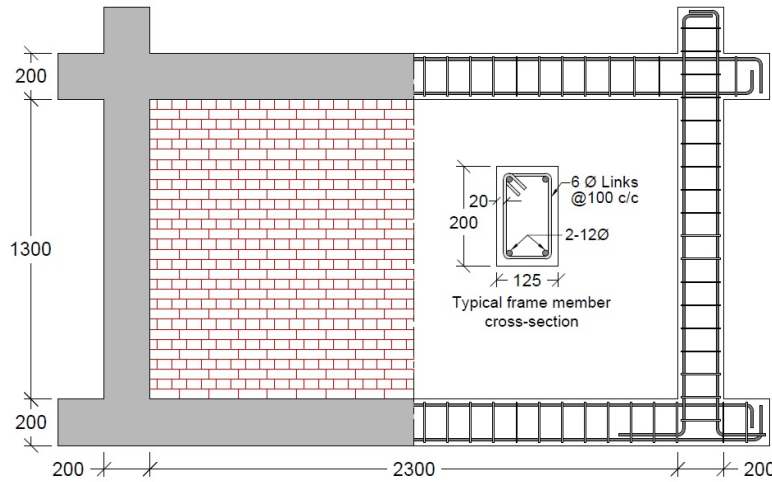


Fig. 1 – Geometric and reinforcement details of the test specimen

Table 1 – FRCM Strengthening configuration for infill wall specimen

No.	Symbol	Fabric type and orientation	Mechanical anchors	Mode of application
1.	CS	No reinforcement (Control Specimen)		
2.	DU <sub>0-90</sub>	Main fabric at 0/90°	No	Direct application
3.	DA <sub>0-90</sub>	Main fabric at 0/90°	Yes	Direct application
4.	SU <sub>0-90</sub>	Main fabric at 0/90°	No	Sandwich application
5.	SA <sub>0-90</sub>	Main fabric at 0/90°	Yes	Sandwich application
6.	DA <sub>45</sub>	Main fabric at +/- 45°	Yes	Direct application

## 2.2 Material Characterization

Specially made half-scale burnt clay bricks (130 mm × 64 mm × 43 mm) and lime-cement mortar mix of 1:1:6 proportion (cement: lime: sand) was used for laying the masonry walls. The physical and mechanical properties of these chosen half-scale bricks correlate well with that of full-scale bricks [12]. The average compressive strength of brick units was 14.4 MPa with a coefficient of variation (COV) of 11.5%. Cement mortar of mix proportion 1:4 (cement: sand) was used for plastering the walls. The average compressive strength of mortar used for masonry and plaster was 8.2 MPa (COV = 16.9%) and 15.0 MPa (COV = 13.6%), respectively. Masonry prisms of five bricks height were made during construction of the brick walls and their average compressive strength was 8.2 MPa (COV = 7.5%). Concrete of mix proportions 1:1.583:2.814 with a water cement ratio of 0.53 was used in RC members of all specimens. The average compressive strength of 150 mm concrete cubes at 28 days was 33.83 MPa (COV = 3.7%). The average yield strength of 12 mm and 6 mm diameter bars were 509 MPa and 430 MPa, respectively.

Two types of FRP sheets/fabrics, namely main/panel and edge fabrics were used for FRCM strengthening. The main fabric was placed on the entire surface of the infill panel with an overlap of 150 mm on the frame, and 300 mm wide strips of edge fabric was placed along the frame and infill interface, with an overlap of 150 mm on either sides of the frame-infill interface. The fabrics consisted of glass fiber strands woven along two orthogonal directions at equal spacing, forming square grids. The size of the grids was about 25 mm and 8 mm for the main

and edge fabrics, respectively. The main fabric had a tensile strength of 45 kN/m along both warp and weft directions, and the edge fabric had a tensile strength of 62 kN/m and 50 kN/m along the warp and the weft directions, respectively. The tensile properties of the FRCM were determined by performing the coupon test. Ten coupons were tested for both the main and edge fabrics, of which five specimen each were tested to determine the tensile properties of the fabric along the primary (warp) and secondary (weft) directions. The dimensions were fixed based on the guidelines of AC 434 [13]. The average tensile properties of FRCM coupons for the main and edge fabric along the warp and weft directions are presented in Table 2.

Table 2 – Mechanical properties of FRCM coupon

Mechanical property	Main fabric		Edge fabric	
	Warp dir.	Weft dir.	Warp dir.	Weft dir.
Area per unit width (mm <sup>2</sup> /mm), $A_f$	0.104	0.096	0.117	0.079
Uncracked modulus of elasticity (GPa), $E_f$	113.5 (26)*	101.2 (25)	180.9 (38)	143.5 (45)
Cracked modulus of elasticity (GPa), $E_{fc}$	30.7 (10)	26.7 (29)	59.4 (13)	29.4 (41)
Tensile stress at transition point (MPa), $f_{ft}$	118.0 (26)	116.1 (20)	99.7 (24)	78.7 (37)
Ultimate tensile strength (MPa), $f_{fu}$	254.4 (12)	261.6 (12)	286.3 (19)	208.4 (13)
Tensile strain at transition point, $\varepsilon_{ft}$	0.0011 (49)	0.0008 (12)	0.0006 (47)	0.0006 (45)
Ultimate tensile strain, $\varepsilon_{fu}$	0.0063 (9)	0.0067 (21)	0.0036 (19)	0.005 (32)

\*Figure in brackets indicate percentage COV

### 2.3 Fabrication of Test Specimen and FRCM Strengthening

The constructed RC frame was infilled with half-scaled burnt clay brick masonry in running bond flush with the front surface of the frame. The FRCM strengthening was performed after 28 days of curing of the infill wall on the front face of the infill, and the back face was plastered with cement mortar only. The sequence of FRCM strengthening for specimen SA<sub>0-90</sub> after fixing the mechanical anchors at a distance of 75 mm from the frame-infill interface is presented in Fig. 2. The spacing of the mechanical anchors was provided such that the shear capacity of the bolt should exceed the tensile strength of the fabric, in order to prevent the failure of anchors. The spacing of bolts along the length and height of the wall were 165 mm c/c and 175 mm c/c, respectively. Development length of 150 mm was kept for overlapping of main fabric and also beyond the frame and infill boundary as per the guidelines of ACI 549.4R (ACI 2013).

### 3. Test Setup

A unique testing method proposed by Komaraneni et al. [11] and Singhal and Rai [14], was used in the present study for the sequential out-of-plane and in-plane loading. Some modifications were made from the previous setup to facilitate the application of gravity load on columns. The test setup for out-of-plane and in-plane loading is shown in Fig. 3. A 1.8 m × 1.2 m servo-hydraulic driven uniaxial shake table was used for out-of-plane loading. For in-plane loading, a 500 kN servo-hydraulic actuator was used. To simulate boundary conditions for the infilled RC frame, adequate number of lateral supports was provided on both sides of the specimen. The lateral supports were braced at the top to provide torsional restraint to the infill wall during in-plane and out-of-plane loading. The in-plane supports were attached to the strong-reaction floor to transfer overturning loads generated during the in-plane loading without overstressing the shake table bearings. In order to simulate the gravity load, a pre-compression stress of 0.1 MPa was maintained on the wall and a load of 25 kN was applied on columns, using a flexible wire rope arrangement. Artificial mass in form of lead blocks were attached on the wall to simulate the inertial forces generated due to out-of-plane ground motion (Fig. 3).

For the out-of-plane test 17 accelerometers were used, of which 15 were attached to the infill panel, one was placed at the center of top beam and one was attached to the shake table, eight wire potentiometers of stroke

length  $\pm 250$  mm were used for recording the out-of-plane displacement of the infill wall. For in-plane test, five linear variable displacement transducers (LVDTs) were used to record the lateral in-plane displacements at varying heights. Six load cells were used to monitor the pre-compression load on the wall specimen.

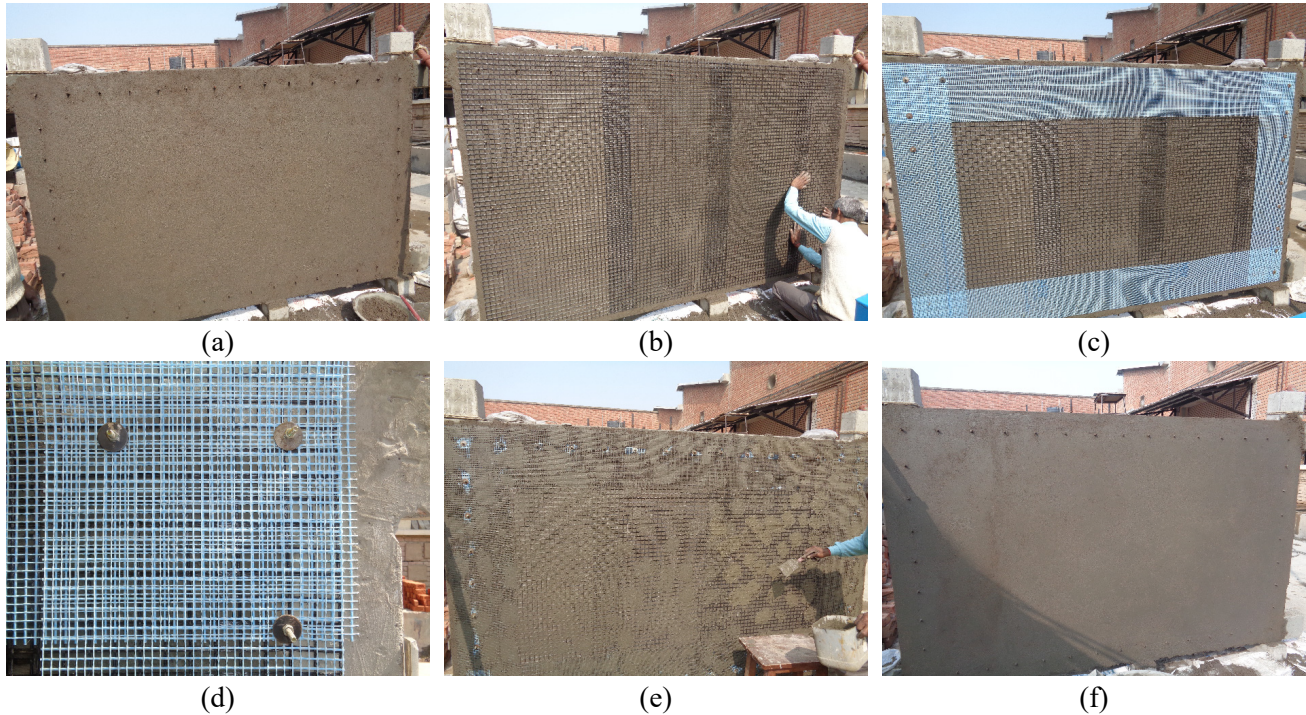


Fig. 2 – Sequence of preparation of plastering of specimen SA<sub>0.90</sub>: (a) application of first layer of 2-3 mm thick plaster, (b) placing of pre-cut main fabric strips with 150 mm overlap, (c) placing of 300 mm wide edge fabric and fastening of mechanical anchors, (d) enlarged view of the mechanical anchors, (e) application of rich cement paste for better bond between the plaster and fabric, and (f) application of second layer of 3-4 mm thick plaster.



Fig. 3 – Typical test setup for wall specimens: (a) out-of-plane loading, and (b) in-plane loading

### 3.1 Loading History and Test Procedure

The specimens were subjected to simulated earthquake ground motions generated by a shake table in the out-of-plane direction. The N21E component of the 1952 Taft earthquake was chosen for the out-of-plane target ground motion, with a PGA of 0.156g. The time axis of the accelerogram was compressed by a factor of  $1/\sqrt{2}$  to satisfy the dynamic similitude relations. The 5% damped response spectra of the Taft motion scaled to a PGA value of

0.4g corresponds well with the design response spectrum for a design earthquake, having a PGA of 0.36g in the Zone V of the Indian Seismic Code IS 1893 [15]. This ground motion is referred as Level V motion. Similarly, the Taft motion is scaled to a corresponding Zone II, III and IV of Indian seismic code and referred as Level II, III, and IV motions, respectively. Also, Level I ground motion was defined as the Taft motion scaled to a PGA of 0.055g. In-plane loading consisted of displacement controlled slow cyclic drifts, which were selected as per the guidelines of ACI 374.05 [16]. The loading history consisted of gradually increasing storey drifts of 0.10%, 0.20%, 0.25%, 0.35%, 0.50%, 0.75%, 1.00%, 1.40%, 1.75%, 2.20% and 2.75%. Each displacement cycle was repeated for three times at each drift ratio.

After safely mounting the specimen on the shake table, the required gravity load was applied. The load test started with the out-of-plane shake table motions consisting of a series of incremental Taft motions from Level I to Level V, with the white noise tests in between. After the completion of this out-of-plane loading schedule, the specimen was subjected to quasi-static in-plane cyclic loading. The in-plane cyclic loading was continued until cracks were visible, which was observed at 0.50% drift cycle for all specimens. After this drift level, the second cycle of out-of-plane loading was applied which consisted of Level V Taft motion only. The second cycle of in-plane loading was performed (drift ratio 0.75%) and the alternate cycles of out-of-plane and in-plane loading was continued until the specimen failed, as shown in Fig. 4. The specimens were subjected to a maximum of 11 in-plane drift levels (DL1 to DL11) and out-of-plane dynamic loads were applied corresponding to seven damage states (DS1 to DS7).

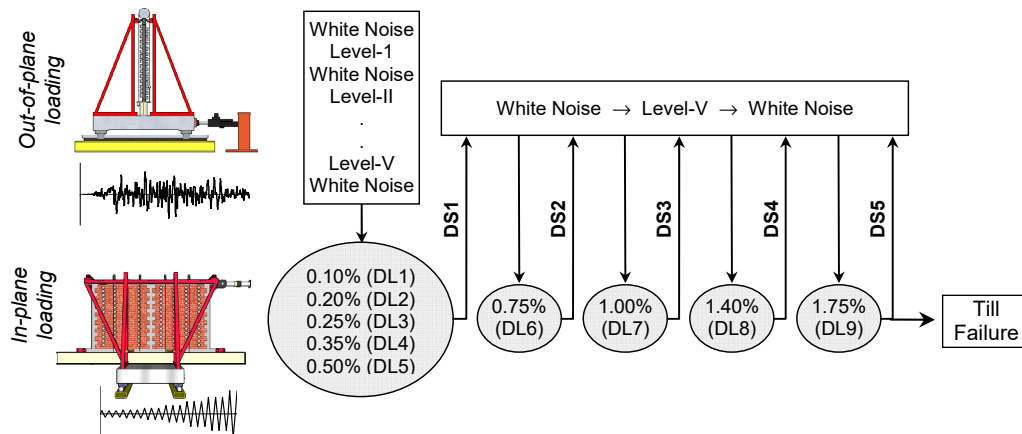


Fig. 4 – Details of loading sequence and test procedure (DL = In-plane drift level and DS = Damage state)

## 4. Results and Discussion

### 4.1 Physical Observations during the Tests

The physical observations made during the test include the description of the cracks formed in the infill wall and frame, damage to the rebars and lateral ties of the columns, performance of FRMC strengthening system and the corresponding variation in the load response. Majority of the cracks were formed during the in-plane loading, while not many new cracks were formed during the out-of-plane loading. The failure patterns of all the specimens are illustrated in Fig. 5.

The infill panel of the control specimen experienced severe cracking, and disintegrated due to its brittle nature. Subsequently, the loosened masonry panels were dislodged from their position under out-of-plane loading, which was further aggravated by the lack of adequate bond between the infill and frame. However, in strengthened specimens, propagation of the cracks on the unstrengthened face of the infill was delayed by the FRMC strengthening, preserving the structural integrity and controlling the excessive out-of-plane deflection.

In the control specimen, CS and the two unanchored specimens, DU<sub>0-90</sub> and SU<sub>0-90</sub>, separation of the infill panel from the frame was observed at a drift level of 0.75%. In these specimens, shear cracks were formed at the

column ends which were characterized by the abrupt drop in the in-plane load capacity. Due to the separation of the infill panels, the loads were primarily resisted by the frame in these specimens, leading to extensive damage to columns in the form of buckling of rebars, fracture of lateral ties and crushing of concrete, while only a few new cracks were formed in the infill panels. Wall SU<sub>0-90</sub> showed poor energy dissipation with formation of plastic hinge at the base of the columns due to the detachment of infill panel from the bottom beam at 1.4% drift level. No cracks were formed in the infill panel of this specimen.

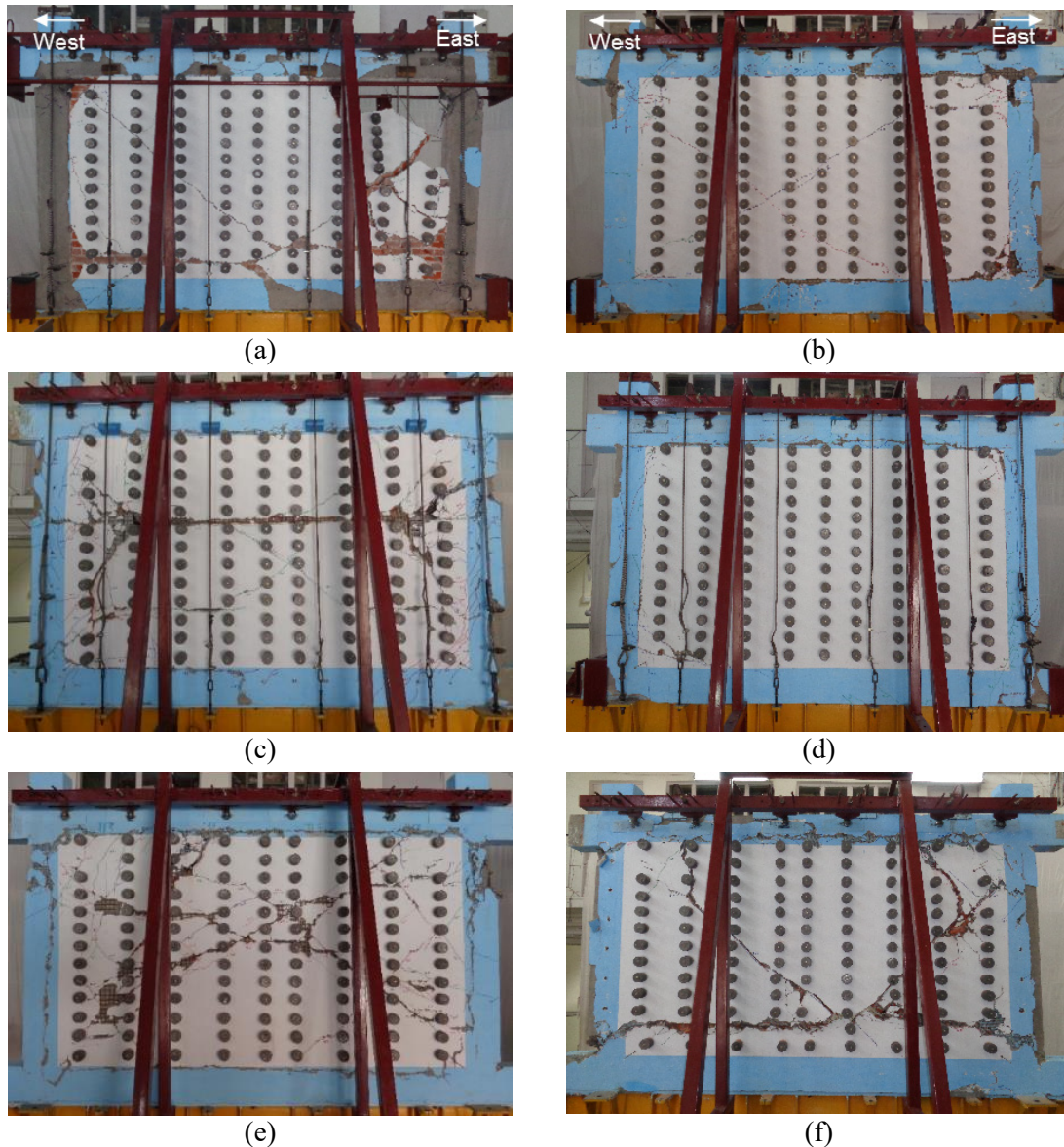


Fig. 5 – Specimen at the end of the test:(a) CS, (b) DU<sub>0-90</sub>, (c) DA<sub>0-90</sub>, (d) SU<sub>0-90</sub>, (e) SA<sub>0-90</sub>, and (f) DA<sub>45</sub>

In the anchored specimens with orthogonal orientation of fabric, DA<sub>0-90</sub> and SA<sub>0-90</sub>, the FRCM strengthening system comprising the edge fabric and anchors, was effective in enhancing the frame-infill interaction. The mechanical anchors restricted the tendency of the infill wall to separate from the frame, and assisted in the formation of diagonal strut mechanism with large contact area between the frame and infill, which prevented the concentration of damage at the corners of the infill wall and the column. Shear sliding cracks were formed along the bed-joints at 1.0% and 1.4% drift levels in specimens DA<sub>0-90</sub> and SA<sub>0-90</sub>, respectively. Shear cracks were formed in columns at mid-height as extensions of the bed-joint cracks formed in the infill walls. Since the infills were still in contact with the frame and were resisting the in-plane loads, a well distributed cracking pattern was

observed, along with gradual decrease in the load capacity. The fabric ruptured along the bed-joint and the diagonal cracks were formed in these specimens during the 2.2% and 2.75% drift cycles, however, the out-of-plane stability of these specimens was not jeopardized due to the superior connection of the infill panels with the RC frame. The performances of the specimens DA<sub>0-90</sub> and SA<sub>0-90</sub> were identical up to 2.2% drift cycle, however, in the last in-plane loading cycle, the infill panel of the specimen SA<sub>0-90</sub> experienced more damage compared to DA<sub>0-90</sub>, due to the debonding of fabric from the surface of masonry.

The fabric of specimen DA<sub>45</sub> experienced overstressing due to its oblique orientation, which was evident from the formation of cracks around the anchors during 0.5% drift cycle. The infill separated from the frame at 0.75% drift level, which resulted in the formation of shear cracks at column ends and a sudden drop in the in-plane strength. Though bed-joint crack was formed, the specimen was ineffective in resisting the stresses due to sliding of masonry, and experienced extensive rupture of fabric and walking-out of infill by about 20 mm during the 2.2% and 2.75% drift cycles.

From the physical observations, it was evident that the direct application was superior to the sandwich application in preventing the debonding of fabric. The mechanical anchors improved the efficiency of the strengthening system by improving the bond of infill panel with the surrounding frame. The oblique orientation of fabric was not as effective as the orthogonal orientation, as it led to overstressing of the fabric.

#### 4.2 Out-of-Plane Behavior of Damaged Walls

The variation of equivalent uniform pressure (calculated from observed inertia forces) and peak out-of-plane displacements of the infill panels with respect to different in-plane drift levels are shown in Figs. 6a and 6b, respectively. Uniform out-of-plane pressure was calculated from the value of acceleration experienced by the infill panel. The value of equivalent out-of-plane pressure was obtained as follows: the value of acceleration recorded at each location was multiplied with the corresponding tributary mass to obtain the inertia force and summed over all the locations, which was then divided by the wall area. The acceleration values were taken at the instant at which the accelerometer at the center of the infill wall experienced maximum acceleration.

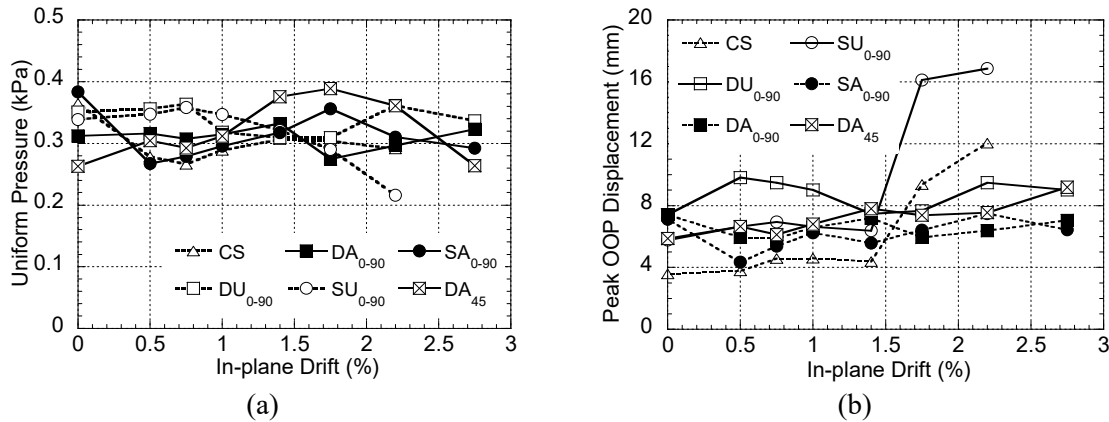


Fig. 6 – (a) Variation of peak uniform pressure and (b) out-of-plane displacement with different in-plane drift levels (damage)

The uniform out-of-plane pressure and displacement remained almost constant in all the walls up to 1.4% drift level. The out-of-plane pressure in the specimens CS, SU<sub>0-90</sub> and DA<sub>45</sub> showed a sharp decline after 1.75% and 2.2% in-plane drift cycles (Fig. 6a). The stiffness degradation of these specimens, as a result of damage accumulation under in-plane loads was responsible for the drop in the observed out-of-plane acceleration. However, the specimens DU<sub>0-90</sub>, DA<sub>0-90</sub> and SA<sub>0-90</sub> preserved structural integrity without significant change in the out-of-plane stiffness till the end of the test, and hence the out-of-plane pressure remained almost constant.

Higher out-of-plane displacements of about 12 mm were observed in specimen CS due disintegration of the infill panel and 16 mm in the specimen SU<sub>0-90</sub> due to detachment of the infill panel from the bottom beam,

respectively (Fig. 6b). The out-of-plane displacement was comparatively lesser in rest of the strengthened specimens. Walls DU<sub>0-90</sub> and DA<sub>45</sub> preserved structural integrity, and experienced peak out-of-plane displacements of about 9 mm. Though the infill panel of walls DA<sub>0-90</sub> and SA<sub>0-90</sub> suffered extensive cracks under in-plane loading, the out-of-plane displacements were below 8 mm due to the limited separation of the infill panel from the frame.

### 4.3 In-Plane Load Displacement Response

The in-plane behavior of the infill wall has been evaluated in terms of the peak load capacity, displacement ductility and strength degradation. The summary of the in-plane response for the test specimens is presented in Table 3. The hysteretic response of all specimens with the summary of strengths and key damage observations are shown in Fig. 7. The key damage observations are indicated by the occurrence of various inelastic activities such as, separation of frame and infill wall (S), shear crack in the column (S<sub>c</sub>), buckling of longitudinal rebars (B), fracture of lateral ties in the column (F), rocking of the wall panel (R) and crushing of bricks (C<sub>b</sub>).

Table 3 – Summary of observed response for all specimens

Wall	Ultimate load, $R_{max}$ (kN)	$\delta_y^*$ (%)	$\delta_u^\#$ (%)	Displ. ductility, $\mu_d$	Strength degradation, $C_{sd}$
CS	+228.5 -227.0	+0.23 -0.20	+1.22 -2.19	5.2 (+) 11.0 (-)	0.38 (+) 0.59 (-)
DU <sub>0-90</sub>	+270.2 -264.0	+0.28 -0.30	+1.29 -1.14	4.7 (+) 3.8 (-)	0.50 (+) 0.37 (-)
DA <sub>0-90</sub>	+250.7 -243.5	+0.31 -0.45	+1.29 -1.55	4.1 (+) 3.4 (-)	0.56 (+) 0.57 (-)
SU <sub>0-90</sub>	+251.5 -248.8	+0.25 -0.24	+0.99 -0.80	4.1 (+) 3.3 (-)	0.18 (+) 0.16 (-)
SA <sub>0-90</sub>	+270.0 -287.3	+0.27 -0.27	+1.93 -1.36	7.2 (+) 5.1 (-)	0.36 (+) 0.33 (-)
DA <sub>45</sub>	+292.1 -275.9	+0.35 -0.27	+1.40 -1.20	4.0 (+) 4.5 (-)	0.33 (+) 0.39 (-)

\*  $\delta_y$  = drift ratio at yield displacement

#  $\delta_u$  = drift ratio at post-peak displacement corresponding to  $R_w$  i.e., 80% of peak load

Idealized tri-linear plots have been developed from the experimental load-deformation envelope, which facilitate in obtaining the parameters for comparing the performance of the different wall specimens. Generally, for calculating the displacement ductility of a specimen, the yield displacement is taken corresponding to the yielding of vertical reinforcement. However from design considerations, the yield point is defined based on the system behavior. In the present study, ductility is determined from the experimental load-deformation envelope. The results are presented for the specimens in the positive and negative directions separately, due to the asymmetric response observed in some of the wall specimens (Table 3 and Fig. 7). The tri-linear plot has been plotted by defining three limit states [17], as follows:

1. Cracking limit, defined using the point corresponding to load  $R_{cr}$  and displacement  $\delta_{cr}$  which represents the change of slope of the backbone curve due to the formation of first noteworthy cracks in the wall.
2. Maximum resistance, which is defined using the maximum load  $R_{max}$  and the corresponding displacement  $\delta_{R_{max}}$  attained during the test.
3. Ultimate state, defined by the ultimate displacement  $\delta_{max}$  and the corresponding residual strength,  $R_r$ .

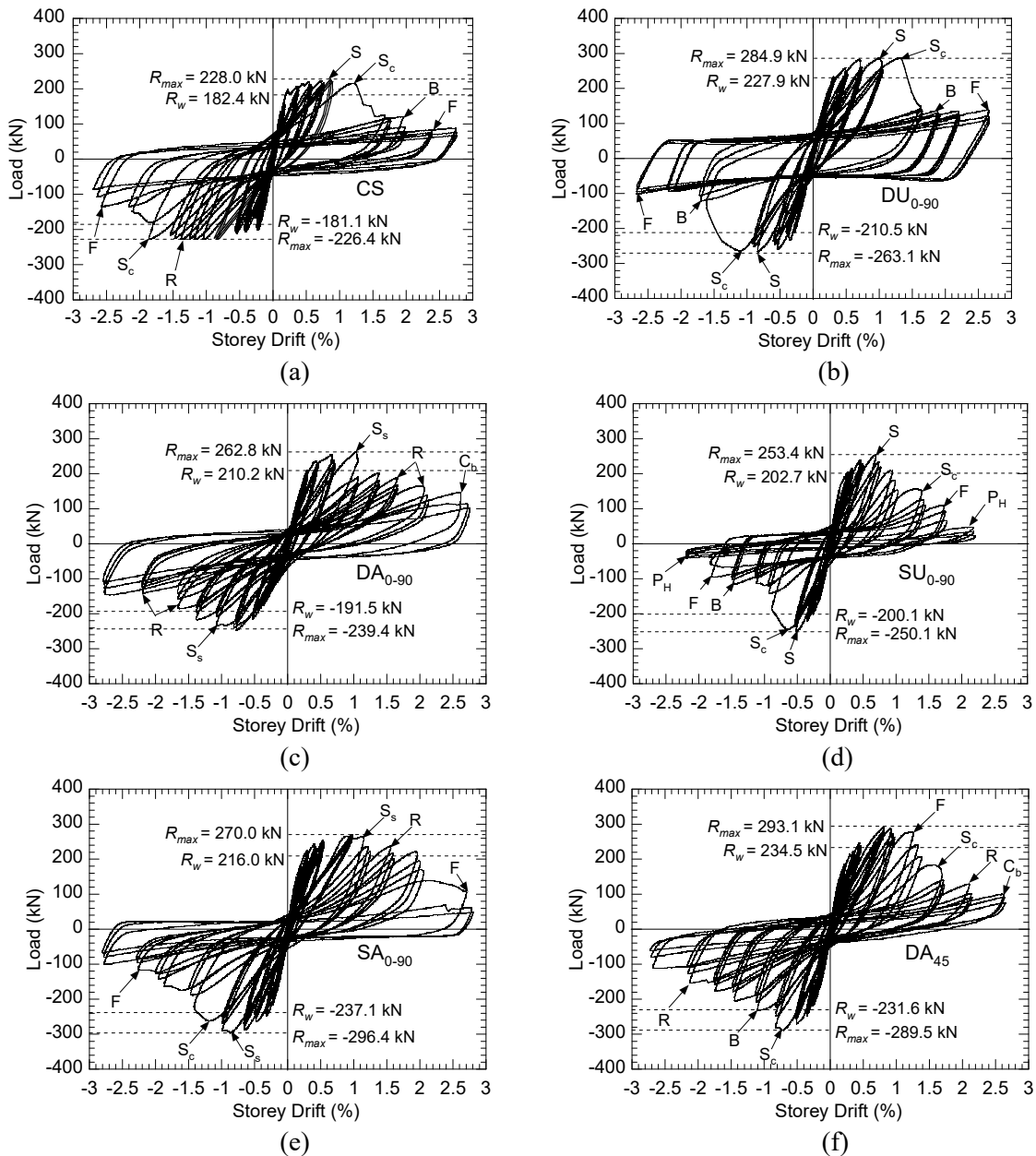


Fig. 7 – Comparison of hysteretic behavior of the specimens (S = Separation at wall to column interface,  $S_c$  = Shear crack in the column, B = Buckling of column rebars, F = Fracture of lateral tie in column, R = Rocking of masonry panel and,  $P_H$  = Plastic hinging at the column ends and  $C_b$  = Crushing of brick)

In addition to the above limit states, a strength indicator  $R_w$  is defined which indicates the safe working load. The value of  $R_w$  is taken as 80% of the peak load and the corresponding displacement in the post-peak regime is defined as  $\delta_u$ . A possible choice of cracking resistance  $R_{cr}$  is  $0.75 R_u$  [18], where  $R_u = 0.9 R_{max}$ . The yield displacement is defined as,  $\delta_y = 0.9 R_{max}/K_e$ . Displacement ductility,  $\mu_d$ , is computed from the ratio of post-peak displacement  $\delta_u$  to yield displacement  $\delta_y$ . To indicate the deterioration in the strength of the wall after reaching peak strength, a strength degradation factor  $C_{sd}$  is used, which is given by the ratio of  $R_r$  to  $R_{max}$ .

The idealized tri-linear plots were obtained from the defined limit states for positive and negative directions separately (Figs. 8a and 8b). The control specimen showed an average in-plane load capacity of 227.2 kN, and for the strengthened specimens the load capacity varied from 247.1 kN to 284.0 kN. The formation of shear cracks in the columns of the specimen CS, and  $SU_{0-90}$  caused due to the poor infill-frame interaction which

resulted in abrupt drop in the load capacity. Wall DA<sub>0-90</sub> showed maximum yield displacement of 4.7 mm (0.31% drift) and 6.7 mm (0.45% drift) along the positive and negative directions, which was consistent with the physical observations of the wall where the onset of cracking was considerably delayed. The anchored specimens exhibited a gradual decrease in load capacity compared to the unanchored specimens, and specimen DA<sub>0-90</sub> showed a superior performance with symmetric response along both the directions of loading and exhibited highest residual strength (Fig. 8). Specimen DA<sub>0-90</sub> showed the highest strength degradation factor ( $C_{sd}$ ) of 0.56 and 0.57 in the positive and negative directions, respectively. In contrast, specimen SU<sub>0-90</sub> had least strength degradation factor of 0.16 and 0.18.

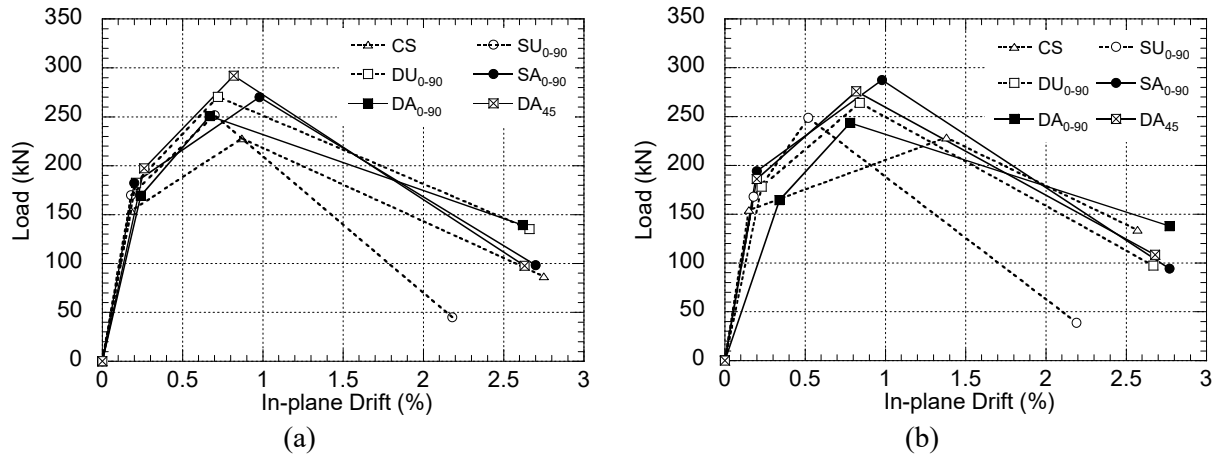


Fig. 8 – Idealized tri-linear load displacement relationship for the infill wall specimens: (a) positive direction, and (b) negative direction

#### 4. Conclusions

This study was concerned with the evaluation of out-of-plane strength of FRCM strengthened half-scale masonry infill walls with in-plane damage. Strengthened specimens were observed to maintain structural integrity and out-of-plane stability under design level out-of-plane inertial forces even in the damage state caused by in-plane storey drifts in excess of 2.0%. The FRCM strengthening was effective in improving the in-plane and out-of-plane behavior of the infill wall.

The specimen strengthened with direct mode of application, which is easier to implement in practice had a better performance compared to sandwich application. In direct application, fabric was in contact with masonry during high in-plane drift cycles and hence the provided reinforcement reduced the extent of damage in the infill. However, in sandwich application, flaking of plaster resulted in the debonding of fabric from the surface of masonry, which aggravated the extent of damage in the infill panel, leading to a poor out-of-plane performance.

The mechanical anchors were helpful in limiting the separation of the infill wall from the frame. This resulted in better interaction between the wall and the frame in resisting the in-plane forces, and also preserving the stability under out-of-plane loads. The anchored specimens exhibited better energy dissipation due to the formation of well distributed cracks in the infill panel and lesser damage to the surrounding RC frame. The mechanical anchors could also effectively control the excessive out-of-plane displacements though the infill panels were severely damaged under in-plane loading. Extensive damage was observed in the specimen having oblique orientation of the fabric with anchors, due to overstressing of the fabric and the strengthening proved to be ineffective in resisting the stresses after the formation of shear sliding cracks.

#### 5. Acknowledgements

Authors would like to acknowledge Saint Gobain Research India Pvt. Ltd for providing fiber composite materials for FRCM strengthening of masonry. Any opinions, findings, and conclusions or recommendations



expressed in this material are those of the authors and do not necessarily reflect the views of the Saint Gobain Research India.

## 6. References

- [1] Tumialan JG, Galati N, Nanni A (2003): Fiber-reinforced polymer strengthening of unreinforced masonry walls subject to out-of-plane loads. *ACI Structural Journal*, **100** (3), 312–329.
- [2] Silva PF, Yu P, Nanni A (2008): Monte carlo simulation for validating the in-plane shear capacity of URM walls strengthened with GFRP grid reinforced polyurea. *Journal of Composites for Construction*, **12** (4), 405–415.
- [3] Almusallam TH, Al-Salloum YA (2007): Behavior of FRP strengthened infill walls under in-plane seismic loading. *Journal of Composites for Construction*, **11** (3), 308–318.
- [4] Papanicolaou CG, Triantafillou TC, Karlos K, Papathanasiou M (2007): Textile reinforced mortar (TRM) versus FRP as strengthening material of URM walls: In-plane cyclic loading. *Materials and Structures*, **40** (10), 1081–1097.
- [5] Papanicolaou CG, Triantafillou TC, Papathanasiou M, Karlos K (2008): Textile reinforced mortar (TRM) versus FRP as strengthening material of URM walls: Out-of-plane cyclic loading. *Materials and Structures*, **41** (1), 143–157.
- [6] Babaeidarabad S, De Caso F, Nanni A (2013): URM walls strengthened with fabric-reinforced cementitious matrix composite subjected to diagonal compression. *Journal of Composites for Construction*, 04013045-1-9.
- [7] Babaeidarabad S, De Caso F, Nanni A (2014): Out-of-plane behavior of URM walls strengthened with fabric-reinforced cementitious matrix (FRCM) composite. *Journal of Composites for Construction*, 04013057.
- [8] Prota A, Marcari G, Fabbrocino G, Manfredi G, Aldea C (2006): Experimental in-plane behavior of tuff masonry strengthened with cementitious matrix–grid composites. *Journal of Composites for Construction*, **10** (3), 223–233.
- [9] Parisi F, Iovinella A, Balsamo A, Augenti N, Prota A (2013): In-plane behavior of tuff masonry strengthened with inorganic matrix–grid composites. *Composites Part B: Engineering*, **45** (1), 1657–1666.
- [10] Koutas L, Bousias SN, Triantafillou TC (2014): Seismic strengthening of masonry-infilled RC frames with TRM: Experimental study. *Journal of Composites for Construction*, **19** (2), 04014048.
- [11] Komaraneni S, Rai DC, Singhal V (2011): Seismic behavior of framed masonry panels with prior damage when subjected to out-of-plane loading. *Earthquake Spectra*, **27** (4), 1077–1103.
- [12] Singhal V, Rai DC (2013): Suitability of half-scale burnt clay bricks for shake table tests on masonry walls. *Journal of Materials in Civil Engineering*, **26** (4), 644–657.
- [13] AC434. (2013): *Acceptance criteria for masonry and concrete strengthening using fiber-reinforced cementitious matrix (FRCM) composite systems*. ICC Evaluation Service, Whittier, CA
- [14] Singhal V, Rai DC (2014): Role of toothing on in-plane and out-of-plane behavior of confined masonry walls. *Journal of Structural Engineering*, 04014053-1-14.
- [15] Bureau of Indian Standards (BIS). (2002): *Indian standard criteria for earthquake resistant design of structure, Part 1: General provisions and buildings*, IS 1893, 5th Rev., New Delhi, India.
- [16] American Concrete Institute (ACI). (2005): *Acceptance criteria for moment frames based on structural testing and commentary*. ACI 374.1-05, ACI Committee 374, Farmington Hills, MI.
- [17] Tomažević M, Klemenc I (1997): Seismic behavior of confined masonry walls. *Earthquake Engineering and Structural Dynamics*, **26** (10), 1059–1071.
- [18] Magenes G, Calvi G (1997): In-plane seismic response of brick masonry walls. *Earthquake Engineering and Structural Dynamics*, **26** (11), 1091–1112.